

Effects of bone marrow mesenchymal stem cell-derived exosomes on bone formation on titanium

Xiaoling Zhang

Qinghai Provincial People's Hospital

Liangzhi Du

Xi'an Medical University; Xi'an Jiaotong University

Ningbo Zhao

Xi'an Medical University; Xi'an Jiaotong University

Lizhe Zhu

Xi'an Medical University; Xi'an Jiaotong University

Lei Wang

Xi'an Medical University; Xi'an Jiaotong University

Xiaofeng Chang (✉ changxf126@126.com)

Xi'an Medical University; Xi'an Jiaotong University <https://orcid.org/0000-0002-1631-5862>

Research article

Keywords: bone marrow mesenchymal stem cell, exosomes, bone formation, titanium

Posted Date: November 5th, 2020

DOI: <https://doi.org/10.21203/rs.3.rs-84302/v1>

License:  This work is licensed under a Creative Commons Attribution 4.0 International License.

[Read Full License](#)

Abstract

Background: In recent years, researchers have found that exosomes, an important component of intercellular signal transduction and exchange, have great significance in bone tissue repair. In this study, to further promote the development of oral implants, preliminary in vitro experiments were conducted to verify the different concentrations of exosomes from bone marrow mesenchymal stem cells (BMSC-exos) for osteogenesis on the surfaces of titanium sheets.

Methods: In this experiment, rabbit bone marrow mesenchymal stem cells (BMSCs) were seeded on the surfaces of 10 mm × 10 mm × 1 mm square titanium sheets and were divided into four groups to investigate their adsorption, proliferation and osteogenesis after treatment with different concentrations of BMSC-exos: 1. BMSCs + titanium + 0 µg/ml BMSC-exos; 2. BMSCs + titanium + 10 µg/ml BMSC-exos; 3. BMSCs + titanium + 25 µg/ml BMSC-exos; and 4. BMSCs + titanium + 50 µg/ml BMSC-exos.

Results: Compared with the control group, BMSCs' adsorption, extension, proliferation and osteogenesis on titanium sheets were significantly increased in the Exosomes group.

Conclusions: Exosomes can promote the bone formation of BMSCs on titanium plates by promoting adsorption, extension, proliferation, production of alkaline phosphatase (ALP) and type I collagen and mineralization during the osteogenesis process.

Background

Bone formation is a key factor in the success of implants. Promoting the bone formation of implants and bone regeneration around implants is a major problem for researchers. In recent years, bone biomaterials have been the focus of research on implant osseointegration and osteogenesis induction. The goal is to improve and promote osteogenesis by increasing the adsorption, proliferation, and osteogenic-related gene expression of osteogenic cells and osteoblasts on the implant surface.

BMSCs are important for bone formation. Bone formation in the head and face occurs mainly in the form of intramembranous osteogenesis [1]. BMSCs first differentiate into osteoblasts and proliferate and secrete near the bone surface. Substances such as ALP and type I collagen, under the control of many cytokines and pathways, induce mature osteoblasts, eventually resulting in the formation of bone cells embedded in the extracellular matrix (ECM) [2]. Exosomes are small vesicles secreted by almost all cells. Although they are small in size and have a diameter of approximately 40–100 nm, exosomes play a large role in various biological functions. Exosomes have become a popular research topic in the medical field. In the circulatory system, exosomes can promote angiogenesis, and bone marrow mesenchymal stem cells (BMSCs) can secrete exosomes to reduce myocardial ischaemia-reperfusion injury [3]. In the nervous system, exosomes can promote axonal growth [4], and astrocyte-derived exosomes can secrete neuroprotective matrices, protect nerve cells, and promote nerve cell proliferation [5]. In the immune system, exosomes also have an extremely important immunomodulatory effect [6]. Burn GM et al. [7] found that exosomes also played an important role in embryonic development. Moreover, the role of

exosomes in bone tissue is quite significant. Before osteoblast differentiation, osteoblast precursors secrete exosomes to promote osteogenesis.

Presently, mesenchymal stem cell-derived exosomes are widely used in the regeneration and repair of tissue damage. As important osteoblast precursor cells, BMSCs are considered to be the cells with the highest exosome production, and they promote bone injury repair [8–10], nerve damage repair [11–14], skin damage repair [14, 15], and liver damage repair [16, 17]. The role of exosomes secreted by mesenchymal stem cells in the repair of bone damage is reflected mainly in the following activities: 1 promoting cell proliferation and migration; 2 inhibiting apoptosis and inflammation; 3 promoting growth factor expression; and 4 promoting collagen production and angiogenesis. Zhang et al. [18] showed that the role of exosomes in the repair of bone injury is to enhance the osteoinductive activity of β -tricalcium phosphate (β -TCP) through the PI3K/Akt signalling pathway. Furuta and Qin et al. [8, 9] have shown that these changes affect miRNAs in exosomes. Compared with the most commonly used seed cells in bone tissue engineering, exosomes have the following advantages: 1. Exosomes have low immunogenicity and no obvious adverse reactions [19], such as haemolysis reactions and allergic reactions. 2. The nucleic acid and cytokines carried by the exosomes can produce a stronger biological reaction [20]. 3. Exosomes have a long half-life and are widely distributed in various body fluids [21]. 4. Exosomes can be loaded with many gene-like drugs, thus providing many direct and effective methods for gene therapy [22–24]. 5. Exosomes can be stored at $-20\text{ }^{\circ}\text{C}$ for 6 months without altering their biological activity, thus giving them the advantage of being easy to store and transport [25].

The significant role of BMSC-derived exosomes in the field of bone repair has also brought new opportunities for the oral field. Research on the secretion of exosomes from BMSCs in the periodontal tissue or dental pulp has also made significant progress [26, 27]. On this basis, and to further promote the development of oral implants, this study used preliminary in vitro experiments to verify the adsorption, spread, proliferation and osteogenesis of exosomes derived from BMSCs on implants. For providing an experimental basis for the further study of exosomes secreted by BMSCs during bone formation and osseointegration around the oral implants, and also for providing new clues to treat the bone defects around oral implants and other related diseases.

Methods

Animals

Ten New Zealand white rabbits (2 months years old, male, Shaanxi province, China) weighing from 1-1.5 kg were used in this study. The animals were kept in individual cages within a standard laboratory environment (temperature $23\text{ }^{\circ}\text{C} \pm 3\text{ }^{\circ}\text{C}$, humidity $55\% \pm 15\%$, and ventilation 10 to 20 times/hour). All animals were fed a standard laboratory pellet diet with free access to water. All procedures related to the animals were approved by the Institutional Animal Care and Use Committee at the animal center, department of medicine, Xi 'an Jiaotong university (approval No.1915 – 704; Shaanxi province, China).

After the bone marrow was extracted, the rabbits were unconscious, then all the rabbits were injected 1.5% pentobarbital at 2 ml/kg into the ear vein to anesthetic for euthanized.

Materials

Ti sheets (99.9% purity) were cut into square pieces (1 mm × 10 mm × 10 mm) for the in vitro studies. The specimens were cleaned ultrasonically in deionized water for 30 min, sterilized at high temperature and high pressure, and both sides were exposed to a UV lamp for half an hour. The specimens were divided into four groups: (1) control group (BMSCs + titanium); (2) 10 µg/ml BMSCs-exos + BMSCs + titanium; (3) 25 µg/ml BMSCs-exos + BMSCs + titanium; and (4) 50 µg/ml BMSCs-exos + BMSCs + titanium. For the experiments, the specimens were all cultured in a 24-well plate at 37 °C and 5% CO₂ in a constant-temperature incubator.

Methods

BMSC culture and identification

After fixation, the rabbits were injected 1.5% pentobarbital at 2 ml/kg into the ear vein to anesthetic. The concave part of the inner side of the femur was used for the puncture site. Sterile gloves were worn, the puncture point was determined, and a number 12 bone marrow puncture needle was used to puncture a point from the skin to the periosteum. A syringe pump was slowly connected to the bone marrow tissue, and the bone marrow was extracted, than the rabbits were euthanized by intravenous injection of 100 mg pentobarbital at the ear edge. The bone marrow was then quickly injected into a sterile anticoagulant tube containing heparin (Sanli, Jiangsu, China) and was suspended in complete culture medium (Dulbecco's modified Eagle's medium((DMEM), Gibco) containing 10% foetal bovine serum (FBS) (Gibco) and stored at 37 °C and 5% CO₂ in a constant-temperature incubator for culturing. The first medium change was performed after 48 h. Then, the medium was changed every 2–3 days. Approximately 10 days later, the cells grew to 80–90% confluency and were passaged. Unless otherwise specified, the cells were cultured with normal medium (DMEM containing 10% FBS) and seeded on the specimens at a density of 3×10^4 cells/well.

Flow cytometry was used to identify the surface markers of third generation rabbit BMSCs. There is no specific identification marker for BMSCs, but because BMSCs are non-hematopoietic stem cells, they do not express the surface markers of hematopoietic stem cells such as CD-34, CD-14 and CD45, but express their own marker, CD-44. We detected CD34-PE (NeoBioscience GTX5741), CD14-PE (Abcam ab186689), CD45-PE (NeoBioscience GTX5741) and CD44-FITC (Novus nbp2-22530apc) by flow cytometry. Osteogenic differentiation of the BMSCs was induced with osteogenic medium (normal culture medium containing 10 mM β-glycerophosphate (Sigma), 50 µg/ml ascorbic acid (Sigma), and 10 nM dexamethasone (Sigma)) when the third generation cells grew to 90% confluency. BMSCs were concomitantly induced with adipogenic medium (1 µM dexamethasone (Sigma), 1 mM pyruvate (Sigma), 2 mM L-glutamine (Sigma), 0.5 M isobutyl methylxanthine (Sigma) and 10 µM insulin (Sigma)). Both the

osteogenic and adipogenic experiments were used to identify the multidirectional differentiation potential of the BMSCs.

BMSC culture and identification

In this experiment, a differential ultracentrifuge (Optima, L-100XP) was used to extract the rabbit BMSC-exos. For exosome extraction from the 3rd generation BMSCs, cells grown to approximately 80% confluency were cultured with DMEM containing 10% non-exosome FBS (the bottom 10% was removed from the FBS after centrifugation at 120,000 g for 14 h at 4 °C). After 24 h, the cell supernatant was collected, and 50 ml of the pre-extracted cell supernatant was centrifuged at 300 g for 10 min and 2000 g at 4 °C. The following steps were carried out: centrifugation for 10 min, discard the pellet, centrifugation at 10,000 g for 30 min, discard the pellet, centrifugation at 100,000 g for 70 min, discard the supernatant, resuspension in 30 µl of Phosphate Buffer solution(PBS), centrifugation at 100,000 g for 70 min, and resuspension in 100 µl of PBS. Finally, the sample was transferred to an EP tube and stored at -80 °C until use.

Analysis of BMSC-exo morphology by field emission scanning electron microscopy(FE-SEM)

The morphology of the BMSC-exos was identified by FE-SEM. The obtained exosome sample was resuspended in 100 µl PBS, and 10 µl drops were pipetted on a 2 mm sample copper net for 1 min. The floating liquid was absorbed with filter paper, and the sample was counterstained at room temperature for 5 min with 3% phosphotungstic acid. Filter paper was used again to absorb the floating liquid, and the sample was washed 1–2 times with double-deionized water and dried at room temperature. FE-SEM imaging was performed at 80 kV-120 kV, and 20 exosomes were selected randomly to measure their diameter. Exosome morphology was identified.

Western blot analysis Western blot analysis was performed to identify the BMSC surface markers/antigens CD63, Hsp70 and Alix. Western blot was done with Wes instrument (WES, WS2494), and the following parameters were set: the separation glue was extracted for 200 s, the concentrated glue was absorbed for 15 s, the sample uptake time was 9 s, the electrophoresis time was 25 min, the electrophoresis constant pressure was 375 V, the time of gel clearance was 230 s with 3 washes of 150 s each, the sealing time was 5 min, the incubation time of the primary antibody was 30 min, and the incubation time of the secondary antibody was 30 min to expose the luminescent solution (HDR). Then, the “start” button was clicked to begin the operation.

BMSC-exos effects on BMSC adhesion and stretching on specimens BMSCs were seeded on the specimens and allowed to settle for 0.5, 1, and 4 h. At each time point, the cells on the specimens were carefully moved to a new 24-well plate, rinsed three times with PBS, and fixed in 500 µl 4% paraformaldehyde (PFA) for 15 min per well. The fixative was aspirated, and the cells were rinsed 3 times with PBS for 3 min each time and stained with DAPI (Sigma) for 10 min. BMSCs fixed at time points 1, 4, and 12 h were stained with fluorescein isothiocyanate(FITC) - phalloidin (Sigma) and counterstained with DAPI. Fluorescence images were taken by a fluorescence microscope (Olympus, FSX100). The cell

number and distribution were assessed in five randomly chosen fields captured at 40 × magnification and 400 × magnification. The number of cells was quantified by Image J 1.8.0 software (Rawak Software, Germany, Version 1.8.0).

BMSC-exos for BMSC proliferation on specimens The effect of BMSC-exos on the proliferation of BMSCs on the specimens was assessed using a Cell-Counting Kit 8 (CCK-8, Boster, Wuhan, China). BMSCs were seeded on the specimens and allowed to culture for 24 h, 48 h, and 72 h using medium with BMSC-exos. The medium was changed on the second day. At each time point, the cells on the specimens were carefully moved to a new 24-well plate and rinsed three times with PBS. CCK-8 solution and normal medium were prepared as working solutions at 1:9, and 300 µg of the mixture solution was added to each well. The optical density (OD) of the solution was measured at 450 nm with a microplate reader (Thermo, Shanghai, China).

ALP activity assays The ALP activity of the specimens was assessed qualitatively using a 5-bromo-4-chloro-3-indolyl phosphate (BCIP)/nitro blue tetrazolium (NBT) ALP colour development kit (Beyotime, Shanghai, China). BMSCs were seeded on the specimens at a density of 8×10^4 cells/well. Three days later, the normal medium was changed to BMSC-exo osteogenesis induction medium, and the cells were cultured for 7 days and 14 days. The medium was changed every three days. At each time point, the cells on the specimens were carefully moved to a new 24-well plate and rinsed three times with PBS. Then, the cells were fixed with 4% PFA for 15 min and stained with the working solution for 24 h. After washing 3 times with PBS for 3 min each time, titanium tablets were added dropwise. Two hundred microlitres of the ALP working solution was added to ensure that the working fluid covered the surface of the sample, and the sample was incubated for 24 h at room temperature in the dark. The staining solution was aspirated, and the sample was washed with PBS 2 times to stop the colour development and observe the staining. The stained area was quantified by Image J 1.8.0 software.

Enzyme-linked immunosorbent assay (ELISA) An ELISA was used to determine the secretion of collagen I on the specimen. BMSCs was cultured in the same way former for 7 days and 14 days. At each time point, the cells were moved on 24-well plate seemly. Then, 150 µl of RIPA lysate buffer was added and incubated on ice for 30 min, and the cells were scraped from the titanium sheet with a cell scraper into a sterile EP tube. Then, a rabbit COL-I kit (TSZ, RG01236) was used according to the assay procedure for the calculation of collagen I secretion.

Mineralization assay Mineralization on the specimens was evaluated by Alizarin Red S (Solarbio) staining. BMSCs was cultured in the same way former for 7 days and 14 days. The cells on the specimens were moved seemly on the 24-well plate at each time point. Then, the cells were fixed with 4% PFA and stained with Alizarin Red S for 30 min at room temperature. Then, the cells were rinsed three times with PBS for 5 min each time. The images of the specimens were captured (40 × lens) using an inverted light microscope (Olympus, FSX100).

Statistical expression

The quantitative data are expressed as the mean \pm standard deviation (SD). All quantified results were calculated using ImageJ Software 8.0. All data analysis was carried out using GraphPad Prism 8 software (GraphPad Software, USA, Version 8.0.0). Unless otherwise stated, the p values were calculated using Student's t tests, and the error bars indicate the SD. The significance levels were subdivided into * (p value < 0.05), ** (p value < 0.01), *** (p value < 0.001) and **** (p value < 0.0001). For correlation analysis, Pearson's value was calculated. Statistical analyses were performed by one-way analysis of variance and the Student-Newman-Keuls-q (SNK-q) test using SPSS v14.0 statistical software when comparing the concentration and time correlation.

Results

Cell culture and characterization After primary culture for 24 h, under an inverted microscope, a small number of cells were growing in a circular pattern adhered to the wall. On the 7th day of cell culture, the adhered long, spindle-like cells were observed to grow like colonies under the microscope (Fig. 2Aa). After being subcultured, the cells grew rapidly, reaching 90% confluency at the bottom of the culture flask in approximately 3–5 days; additionally, the cells were in the shape of a long spindle. When the cells were passaged to the third generation, there were fewer hybrid cells (Fig. 2Ab), so these could be used for subsequent experimental studies.

Flow cytometry was performed to detect the P3 surface marker in rabbit BMSCs. The results showed that the rabbit BMSCs had low expression levels of CD34 (0.66%), CD14 (2.57%), and CD45 (1.78%) and high expression levels of CD44 (99.67%)(Fig. 2B). The characteristics of the cultured cells conformed to those of BMSCs. Alizarin red staining of BMSCs after osteogenic induction showed positively(Fig. 2C). Results of oil red O staining in BMSCs induced by lipogenesis showed positively(Fig. 2D).

BMSC-exos characterization BMSC-exos were extracted by ultracentrifugation, and FE-SEM was used to observe their morphology. The results showed that the BMSC-exos had a circular or elliptical disc-like vesicle structure with a diameter of approximately 40–100 nm and a complete membrane structure (Fig. 2E). Western blot assays showed that the BMSC-exos positively expressed CD63, hsp70 and Alix (Fig. 2F). Thus, we successfully isolated BMSC-exos.

Effect of BMSC-exos on the adherence, stretching and proliferation of BMSCs on the specimens After DAPI staining, the adherence of BMSCs treated with BMSC-exos to the specimens was observed under a fluorescence microscope. The qualitatively assessed adsorption of BMSCs treated with BMSC-exos on the titanium plates was significantly higher than that of the control BMSCs (Fig. 3A). Moreover, at the same time, the quantification confirmed that as the concentration increased, the number of BMSCs on the titanium plate increased ($p < 0.05$) (Fig. 3B). These results are consistent with the ImageJ quantification.

CCK-8 assays were used to assess the proliferation and activity of the BMSCs treated with BMSC-exos on the specimens. Compared with the control group, 25 $\mu\text{g/ml}$, 50 $\mu\text{g/ml}$ BMSC-exos showed increased proliferation activity at 24, 48 and 72 h ($p < 0.05$). There was no correlation between time and the

concentration of BMSCs-exos with regard to the proliferation activity of BMSCs on titanium plates (Fig. 3C).

The cytoskeletal protein F-actin was used to assess cell spreading after 1, 4, and 12 h (Fig. 3D). After 1, 4, and 12 h, the cells treated with BMSC-exos show robust F-actin projections on the specimens compared with the control cells. This distinction became even more evident with 12 h of incubation.

Osteogenic activity of BMSCs At 7 and 14 days after osteogenic induction, the staining intensity of ALP was used to confirm the osteogenic activity of BMSCs on the specimens. ALP staining intensity was significantly higher for the titanium plate group than for the control group. In addition, with as the concentration of BMSC-exos increased, the staining intensity of ALP also increased (Fig. 4A). The quantitative analysis further shows that the result and the action were concentration- dependent (Fig. 4B). These differences were statistically significant ($p < 0.05$).

Collagen secretion The amount of type I collagen produced by cells on the titanium plate on the 7th and 14th days after osteogenic induction. The results showed that type I collagen generation levels in the 25 and 50 $\mu\text{g/ml}$ BMSC-exos groups were significantly higher than in the control group at the same times ($p < 0.01$). However, type I collagen generation was not correlated with BMSCs-exos concentration (Fig. 4C).

Mineralization assay Alizarin Red S staining was used to detect osteogenic mineralization. The area of Alizarin Red S staining was significantly higher for cells on the titanium plate than for cells in the control group 21 days after osteogenic induction, and the intensity of Alizarin Red S staining increased with the concentration of BMSC-exos. The group treated with 50 $\mu\text{g/ml}$ BMSCs-exos had almost complete mineralization on the titanium plate (Fig. 4D).

Discussion

There is sufficient research evidence showing that exosomes promote bone regeneration. First, exosomes can promote the osteogenic differentiation of MSCs. Studies have shown that exosomes secreted by monocytes acting on MSCs can trigger the upregulation of two osteogenesis markers, RUNX-2 and BMP-2 [28]. Second, newly formed osteoblasts can also secrete exosomes, which in turn affect osteoprogenitor cells. A group of researchers [29] found that mature osteoblast-derived exosomes can trigger mutations in miRNA expression profiles, which in turn synergistically inhibit Axin1 expression, a novel component of the Wnt signalling pathway. Finally, upregulation of β -catenin leads to enhanced osteogenic differentiation [30]. During the bone reconstruction process, exosomes play vital roles in the processes of bone breaking and osteogenesis. Letret-rich exosomes from osteoblasts can enhance osteogenesis by modulating HMGA2 and AXIN2 [31]. In contrast, osteoclast-derived exosomes act as inhibitors of osteogenesis. Exogenous miR-214-3p is thought to be involved in the inhibition of osteoblast activity by targeting the 3'-untranslated region UTR of the ATF4 mRNA. During fracture healing, bone marrow stem cell-derived exosomes synergistically express MCP-1, MCP-3, SDF-1, angiogenic factors, mRNA, and miRNA to facilitate bone remodeling [22], possibly by upregulating RUNX-2. Osteogenic proteins such as ALP, OCN and OPN promote osteoblast proliferation and differentiation [9].

Based on the abovementioned exosome's positive effects on bone formation, exosomes are expected to be used in the field of oral implants to promote osseointegration around implants and as a good osteoinductive material for guiding bone regeneration. Therefore, this experiment used in vitro experiments to verify the effects of exosomes derived from MSCs on bone formation around implants. In the experiment, a titanium plate was used to replace the implant for modelling, and the adsorption, proliferation and osteogenesis of BMSC-exos on the osteogenic cells on the titanium plate were studied. The experiment is used to simulate the osteogenesis process after implant placement in vivo, mainly simulating the processes of adsorption, extension, proliferation and osteogenic differentiation of osteogenic cells on implants after implant implantation. The results showed that the amount of BMSCs adsorbed on the titanium sheets was increased in the same time period compared with that in the control group, and the adsorption amount increased with the increase of the concentration of BMSCs-exos. The statistical results show that BMSCs-exos can promote the adsorption of BMSCs on titanium tablets and that this adsorption is positively correlated with the concentration. When the adsorption of BMSCs on titanium sheets was detected, the number of BMSCs adsorbed on titanium sheets increased with the increase of BMSCs-exos concentration at 0.5, 1 and 4 h ($p < 0.01$), demonstrating that BMSCs-exos promote the adsorption of BMSCs on titanium sheets and that adsorption is positively correlated with concentration. With the increase of time, the number of cells adsorbed in the 10 and 50 $\mu\text{g}/\text{mL}$ groups did not change significantly, but the number of cells in the control group and the 25 $\mu\text{g}/\text{mL}$ BMSCs-exos group increased with time, and the number of cells adsorbed also increased. There was no correlation with time. When cells were stretched on the titanium sheet, it was observed under the microscope that the excipient-containing group stretched on the titanium sheet more than the control group, indicating that the exosomes had a certain promoting effect on cell elongation. When studying the proliferation of BMSCs on titanium sheets, the proliferation activities of the 25 and 50 $\mu\text{g}/\text{mL}$ BMSCs-exos groups were enhanced at 24, 48, and 72 h compared with that of the control group ($p < 0.05$). There was no significant difference in the proliferative activity from the 10 $\mu\text{g}/\text{mL}$ BMSCs-exos group, and the statistical results showed that BMSCs-exos had no time- and concentration-related effects on the proliferation of BMSCs on titanium. It was demonstrated that BMSCs-exos require a higher concentration for the promotion of BMSC proliferation activity on titanium sheets, which may have also been caused by fewer BMSCs on titanium sheets during the experiment. In the detection of BMSCs-exos osteogenesis of BMSCs on titanium sheets, alkaline phosphatase activity, type I collagen and osteogenic mineralization during BMSC osteogenic differentiation were examined. The results showed that compared with that in the control group, the staining area of alkaline phosphatase was significantly higher on the 7th and 14th day after osteogenic induction in the group containing BMSCs-exos than in the control group, and with the increase of BMSCs-exos concentration, the staining area of alkaline phosphatase also increased ($p < 0.01$), indicating that the promoting effect of BMSCs-exos on alkaline phosphatase activity was positively correlated with the concentration. In detecting type I collagen, an ELISA confirmed that the type I collagen levels produced at 7 and 14 days after osteogenic induction on the titanium plate were 25 and 50 $\mu\text{g}/\text{mL}$, respectively, in the group containing BMSCs-exos. The BMSCs-exos group had significantly higher levels of type I collagen than the control group. The group with the smaller concentration of 10 $\mu\text{g}/\text{mL}$ BMSCs-exos exhibited no significant difference in the formation of type I collagen on titanium tablets, which

indicated that higher concentrations of BMSCs-exos promoted the secretion of type I collagen during osteogenic differentiation of BMSCs on the titanium surface. Finally, mineralization after osteogenic induction was detected by alizarin red staining 21 days after induction. Microscopically, the degree of mineralization was observed to increase with the increase in BMSCs-exos concentration. Thus, it was demonstrated that BMSCs-exos can promote osteogenic differentiation of BMSCs on titanium sheets. The conclusion can be drawn from this experiment that the bone formation of BMSCs on titanium plates is closely related to their paracrine secretion. BMSC-exos can promote bone formation on titanium plates by promoting the adsorption, extension, proliferation and osteogenic differentiation of BMSCs on the surfaces of titanium plates.

This experiment used in vitro experiments to verify the effects of exosomes derived from BMSCs on bone formation around implants. This experiment is also the first to demonstrate the effects of exosomes on bone tissue around oral implants. These findings are expected to be applied to the field of oral implants to solve bone defect problems in the implant area and promote.

Conclusion

Exosomes can promote the bone formation of BMSCs on titanium plates by promoting adsorption, extension, proliferation, production of ALP and type I collagen and mineralization during the osteogenesis process.

Abbreviations

BMSC-exo: exosomes from bone marrow mesenchymal stem cells; BMSCs: bone marrow mesenchymal stem cells; ALP: alkaline phosphatase; COL-I: type I collagen; ECM: extracellular matrix; DMEM: Dulbecco's modified Eagle's medium; FBS: foetal bovine serum; FE-SEM: field emission scanning electron microscopy; PBS: Phosphate Buffer solution; PFA: paraformaldehyde; FITC: fluorescein isothiocyanate; CCK-8: Cell-Counting Kit 8; OD: optical density; BCIP: 5-bromo-4-chloro-3-indolyl phosphate; NBT: nitro blue tetrazolium; *ELISA*: Enzyme-linked immunosorbent assay; SD: standard deviation; SNK-q: Student-Newman-Keuls-q; UTR: 3'-untranslated region

Declarations

Ethics approval and consent to participate

Ethical clearance for this study were approved by the Institutional Animal Care and Use Committee at the animal center, department of medicine, Xi 'an Jiaotong university (approval No.1915-704; Shaanxi province, China).

Consent for publication

Not applicable.

Availability of data and materials

The datasets used and/or analysed during the current study are available from the corresponding author on reasonable request.

Competing interests

The authors declare that they have no competing interests.

Funding

This research was financially funded by corresponding author Xiaofeng Chang. The funder had role in study design, conduct of experiments, data analysis, decision to publish and preparation of the manuscript.

Authors' contributions

XZ performed all the experiments and data analysis and wrote the computer scripts and the manuscript. XC, BL, NZ and LD contributed to the experimental design and wrote the manuscript. LZ, LW and GZ contributed to the data interpretation, statistical analysis, and manuscript revision. All authors read and approved the final manuscript.

Acknowledgements

This research was supported by the Department of Implantology, Xi'an Jiao Tong University Stomatologic Hospital. The authors would also like to thank the platform and equipment provided by the laboratory of the Stomatologic Hospital of Xi 'an Jiaotong university.

Author details

1First People's Hospital of Qinghai Province, Xining City, Qinghai Province 810000, People's Republic of China. 2Department of Oral Implants, Xi'an Jiao Tong University Stomatologic Hospital & College. Xi'an Jiao Tong University School of Medicine, Xi'an City, Shanxi Province 710004, People's Republic of China. 3First Affiliated Hospital, Xi'an Jiao Tong University, Xi'an City, Shanxi Province 710061, People's Republic of China.

References

1. Franz-Odenaal TA. Induction and patterning of intramembranous bone. *Front Biosci (Landmark Ed)*, 16(undefined), 2011; 2734–46. <https://doi.org/10.2741/3882>.
2. Bernhardsson M, Aspenberg P. Osteoblast precursors and inflammatory cells arrive simultaneously to sites of a trabecular-bone injury. *Acta Orthop*. 2018;89(4):457–61. <https://doi.org/10.1080/17453674.2018.1481682>.

3. Arslan F, Lai RC, Smeets MB, Akeroyd L, Choo A, Aguor ENE, Timmers L, van Rijen HV, Doevendans PA, Pasterkamp G, Lim SK, de Kleijn DP. Mesenchymal stem cell-derived exosomes increase ATP levels, decrease oxidative stress and activate PI3K/Akt pathway to enhance myocardial viability and prevent adverse remodeling after myocardial ischemia/reperfusion injury. *Stem Cell Res.* 2013;10(3):301–12. <https://doi.org/10.1016/j.scr.2013.01.002>.
4. Xin H, Ben LYi,B., K Mark., ZYi,W Xinli., Xia S., ZZ Gang., C Michael. Exosome-mediated transfer of miR-133b from multipotent mesenchymal stromal cells to neural cells contributes to neurite outgrowth. *Stem Cells.*2012; 30(7), 1556-64. <https://doi.org/10.1002/stem.1129>.
5. Wang S, Cesca F, Loers G, Schweizer M, Buck F, Benfenati F, Schachner M, Kleene R. Synapsin I is an oligomannose-carrying glycoprotein, acts as an oligomannose-binding lectin, and promotes neurite outgrowth and neuronal survival when released via glia-derived exosomes. *J Neurosci.* 2011;31(20):7275–90. <https://doi.org/10.1523/JNEUROSCI.6476-10.2011>.
6. Raposo G, Nijman HW, Stoorvogel W, Liejendekker R, Harding CV, Melief CJ, Geuze HJ. B lymphocytes secrete antigen-presenting vesicles. *The Journal of experimental medicine.* 1996;183(3):1161–72. <https://doi.org/10.1084/jem>.
7. Burns GW, Brooks KE, Spencer TE. Extracellular Vesicles Originate from the Conceptus and Uterus During Early Pregnancy in Sheep. *Biol Reprod.* 2016;94(3):56. <https://doi.org/10.1095/biolreprod.115.134973>.
8. Furuta T, Miyaki S, Ishitobi H, Ogura T, Kato Y, Kamei N, Miyado K, Higashi Y, Ochi M. (Mesenchymal Stem Cell-Derived Exosomes Promote Fracture Healing in a Mouse Model. *Stem cells translational medicine.* 2016;5(12):1620–30. <https://doi.org/10.5966/sctm.2015-0285>.
9. Qin Y, Wang L, Gao Z, Che G, Zhang C. Bone marrow stromal/stem cell-derived extracellular vesicles regulate osteoblast activity and differentiation in vitro and promote bone regeneration in vivo. *Scientific reports.* 2016;6:21961. <https://doi.org/10.1038/srep21961>.
10. Qi X, Zhang J, Yuan H, Xu Z, Li Q, Niu X, Hu B, Wang Y, Li X. Exosomes Secreted by Human-Induced Pluripotent Stem Cell-Derived Mesenchymal Stem Cells Repair Critical-Sized Bone Defects through Enhanced Angiogenesis and Osteogenesis in Osteoporotic Rats. *International journal of biological science.* 2016;12(7):836–49. <https://doi.org/10.7150/ijbs.14809>.
11. Zhang Y, Chopp M, Liu XS, Katakowski M, Wang X, Tian X, Wu D, Zhang ZG. Exosomes Derived from Mesenchymal Stromal Cells Promote Axonal Growth of Cortical Neurons. *Mol Neurobiol.* 2017;54(4):2659–73. <https://doi.org/10.1007/s12035-016-9851-0>.
12. Huang JH, Yin XM, Xu Y, Xu CC, Lin X, Ye FB, Cao Y, Lin FY. Systemic Administration of Exosomes Released from Mesenchymal Stromal Cells Attenuates Apoptosis, Inflammation, and Promotes Angiogenesis after Spinal Cord Injury in Rats. *J Neurotrauma.* 2017;34(24):3388–96. <https://doi.org/10.1089/neu.2017.5063>.
13. Chen KH, Chen CH, Wallace CG, Yuen CM, Kao GS, Chen YL, Shao PL, Chen YL, Chai HT, Lin KC, Liu CF, Chang HW, Lee MS, Yip HK. Intravenous administration of xenogenic adipose-derived mesenchymal stem cells (ADMSC) and ADMSC-derived exosomes markedly reduced brain infarct

- volume and preserved neurological function in rat after acute ischemic stroke. *Oncotarget*. 2016;7(46):74537–56. <https://doi.org/10.18632/oncotarget.12902>.
14. Fang S, Xu C, Zhang Y, Xue C, Yang C, Bi H, Qian X, Wu M, Ji K, Zhao Y, Wang Y, Liu H, Xing X. Umbilical Cord-Derived Mesenchymal Stem Cell-Derived Exosomal MicroRNAs Suppress Myofibroblast Differentiation by Inhibiting the Transforming Growth Factor- β /SMAD2 Pathway During Wound Healing. *Stem cells translational medicine*. 2016;5(10):1425–39. <https://doi.org/10.5966/sctm.2015-0367>.
 15. Hu L, Wang J, Zhou X, Xiong Z, Zhao J, Yu R, Huang F, Zhang H, Chen L. Exosomes derived from human adipose mesenchymal stem cells accelerates cutaneous wound healing via optimizing the characteristics of fibroblasts. *Scientific reports*. 2016;6:32993. <https://doi.org/10.1038/srep32993>.
 16. Yan Y, Jiang W, Tan Y, Zou S, Zhang H, Mao F, Gong A, Qian H, Xu W. hucMSC Exosome-Derived GPX1 Is Required for the Recovery of Hepatic Oxidant Injury. *Molecular therapy: the journal of the American Society of Gene Therapy*. 2017;25(2):465–79. <https://doi.org/10.1016/j.ymthe.2016.11.019>.
 17. Tan CY, Lai RC, Wong W, Dan YY, Lim SK, Ho HK. Mesenchymal stem cell-derived exosomes promote hepatic regeneration in drug-induced liver injury models. *Stem Cell Res Ther*. 2014;5(3):76. <https://doi.org/10.1186/scrt465>.
 18. Zhang J, Liu X, Li H, Chen C, Hu B, Niu X, Li Q, Zhao B, Xie Z, Wang Y. Exosomes/tricalcium phosphate combination scaffolds can enhance bone regeneration by activating the PI3K/Akt signaling pathway. *Stem Cell Res Ther*. 2016;7(1):136. <https://doi.org/10.1186/s13287-016-0391-3>.
 19. Jiang XC, Gao JQ. Exosomes as novel bio-carriers for gene and drug delivery. *International journal of pharmaceutics*. 2017;521(1–2):167–75. <https://doi.org/10.1016/j.ijpharm.2017.02.038>.
 20. Wu K, Yang Y, Zhong Y, Ammar HM, Zhang P, Guo R, Liu H, Cheng C, Koroscil TM, Chen Y, Liu S, Bihl JC. The effects of microvesicles on endothelial progenitor cells are compromised in type 2 diabetic patients via downregulation of the miR-126/VEGFR2 pathway. *Am J Physiol Endocrinol Metab*. 2016;310(10):E828–37. <https://doi.org/10.1152/ajpendo.00056.2016>.
 21. Kooijmans SA, Vader P, van Dommelen SM, van Solinge WW, Schiffelers RM. Exosome mimetics: a novel class of drug delivery systems. *Int J Nanomed*. 2012;7:1525–41. <https://doi.org/10.2147/IJN.S29661>.
 22. Alvarez-Erviti L, Seow Y, Yin H, Betts C, Lakhali S, Wood MJ. Delivery of siRNA to the mouse brain by systemic injection of targeted exosomes. *Nature biotechnology*. 2011;29(4):341–5. <https://doi.org/10.1038/nbt.1807>.
 23. Rashed H, Bayraktar M, Helal EK, Abd-Allah G, Amero MF, Chavez-Reyes P, A., & Rodriguez-Aguayo C. Exosomes: From Garbage Bins to Promising Therapeutic Targets. *Int J Mol Sci*. 2017;18(3):538. <https://doi.org/10.3390/ijms18030538>.
 24. Koster E, Cardauns H, Oehmichen M, Staak M. Zur Dichte immunreaktiver Zellen in der Milz bei Drogentodesfällen [Density of immunoreactive cells in the spleen in drug fatalities]. *Beiträge zur gerichtlichen Medizin*. 1990;48:67–73.

25. Lai RC, Chen TS, Lim SK. Mesenchymal stem cell exosome: a novel stem cell-based therapy for cardiovascular disease. *Regenerative medicine*. 2011;6(4):481–92.
<https://doi.org/10.2217/rme.11.35>.
26. Huang CC, Narayanan R, Alapati S, Ravindran S. Exosomes as biomimetic tools for stem cell differentiation: Applications in dental pulp tissue regeneration. *Biomaterials*. 2016;111:103–15.
<https://doi.org/10.1016/j.biomaterials.2016.09.029>.
27. Elalfy MA, Boland PJ, Healey JH. Chemotherapy Curtails Bone Formation From Compliant Compression Fixation of Distal Femoral Endoprostheses. *Clin Orthop Relat Res*. 2019;477(1):206–16. <https://doi.org/10.1097/CORR.0000000000000512>.
28. Li D, Liu J, Guo B, Liang C, Dang L, Lu C, He X, Cheung HY, Xu L, Lu C, He B, Liu B, Shaikh AB, Li F, Wang L, Yang Z, Au DW, Peng S, Zhang Z, Zhang BT, Pan X, Qian A, Shang P, Xiao L, Jiang B, Wong CK, Xu J, Bian Z, Liang Z, Guo DA, Zhu H, Tan W, Lu A, Zhang G. Osteoclast-derived exosomal miR-214-3p inhibits osteoblastic bone formation. *Nature communications*. 2016;7:10872.
<https://doi.org/10.1038/ncomms10872>.
29. Wang X, Guo B, Li Q, Peng J, Yang Z, Wang A, Li D, Hou Z, Lv K, Kan G, Cao H, Wu H, Song J, Pan X, Sun Q, Ling S, Li Y, Zhu M, Zhang P, Peng S, Xie X, Tang T, Hong A, Bian Z, Bai Y, Lu A, Li Y, He F, Zhang G, Li Y. miR-214 targets ATF4 to inhibit bone formation. *Nature medicine*. 2013;19(1):93–100.
<https://doi.org/10.1038/nm.3026>.
30. Sun W, Zhao C, Li Y, Wang L, Nie G, Peng J, Wang A, Zhang P, Tian W, Li Q, Song J, Wang C, Xu X, Tian Y, Zhao D, Xu Z, Zhong G, Han B, Ling S, Chang YZ, Li Y. Osteoclast-derived microRNA-containing exosomes selectively inhibit osteoblast activity. *Cell discovery*. 2016;2:16015.
<https://doi.org/10.1038/celldisc.2016.15>.
31. Raposo G, Tenza D, Mecheri S, Peronet R, Bonnerot C, Desaymard C. Accumulation of major histocompatibility complex class II molecules in mast cell secretory granules and their release upon degranulation. *Molecular biology of the cell*. 1997;8(12):2631–45.
<https://doi.org/10.1091/mbc.8.12.2631>.

Figures

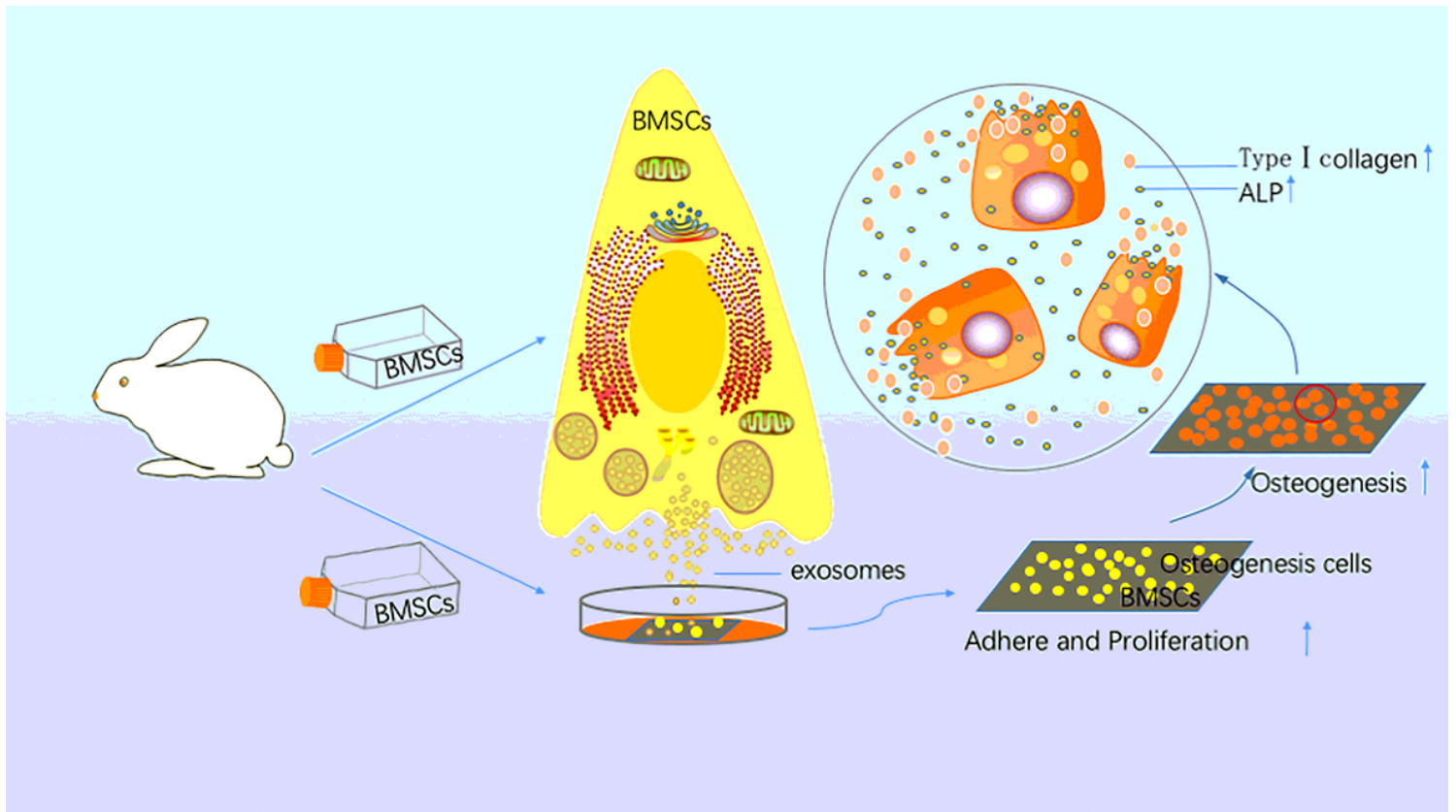


Figure 1

Summary and the mechanism of the experiment (This figure was made by authors of this article) . Rabbit BMSCs were cultured in vitro, some to extract exosomes, some on titanium sheets. The extracted exosomes were added to the BMSCs-titanium sheet complex at different concentrations. The results showed that the exosomes could promote the adsorption, proliferation and osteogenesis of BMSCs in the end on the titanium sheet. And promoted the Alkaline phosphatase (ALP) and Collagen- α in the process of osteogenesis

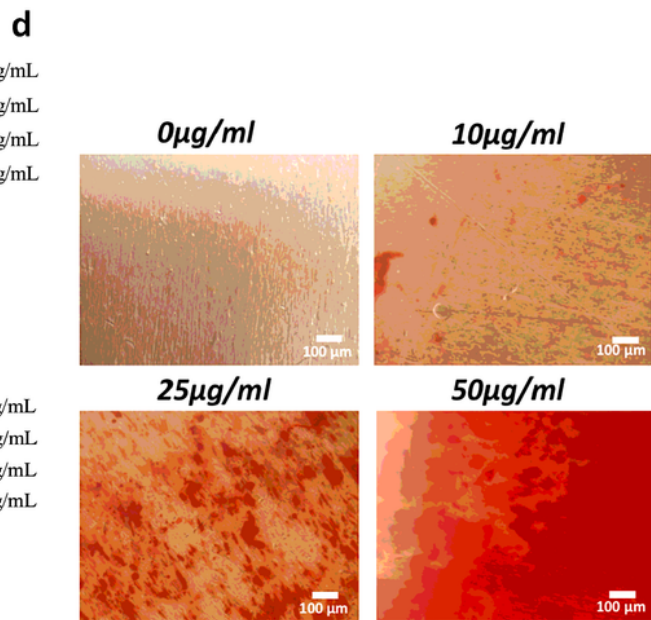
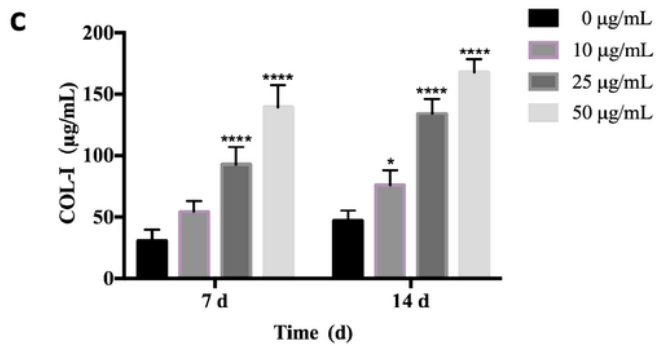
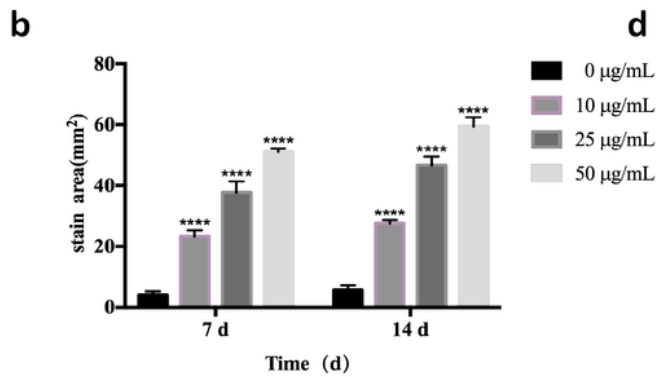
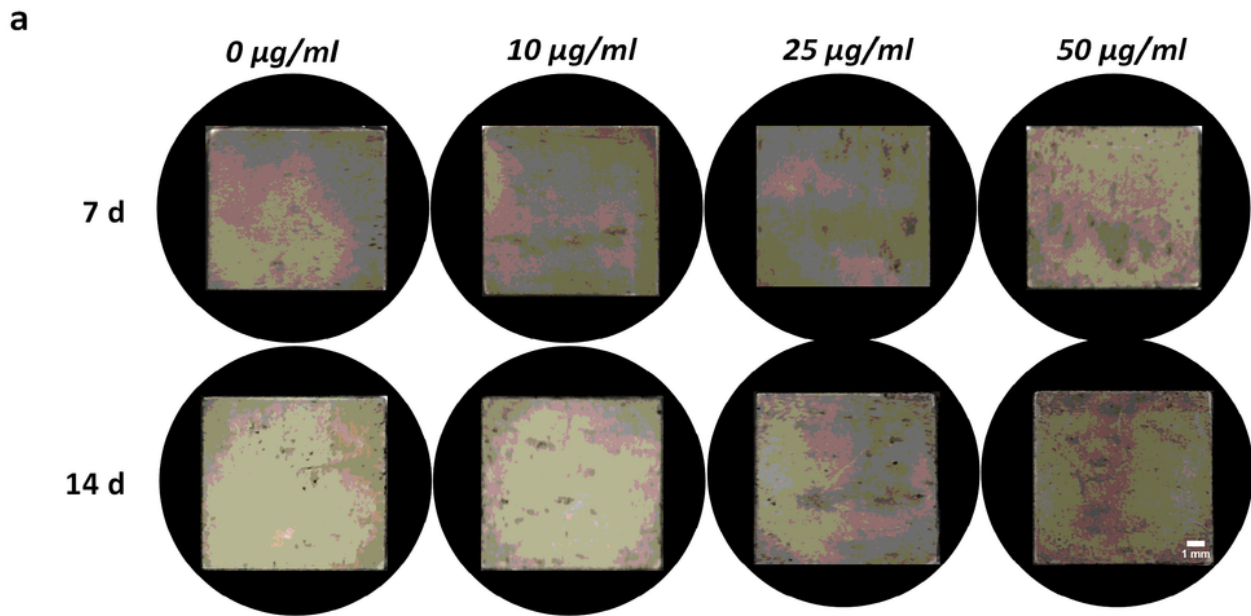


Figure 2

BMSCs and Exosome characterization. a Morphological appearance of cultured BMSCs(bar = 100 µm). b Flow cytometry for the detection of BMSCs surface markers: CD34 and CD44. c Alizarin red staining of BMSCs after osteogenic induction(bar = 100 µm). d Results of oil red O staining in BMSCs induced by lipogenesis(bar = 100 µm). e Morphological analysis of BMSCs-exos by transmission electron

microscopy (bar = 100 nm). f Western blot assay indicated the positive expression of CD63, hsp70 and Alix proteins in BMSCs-exos

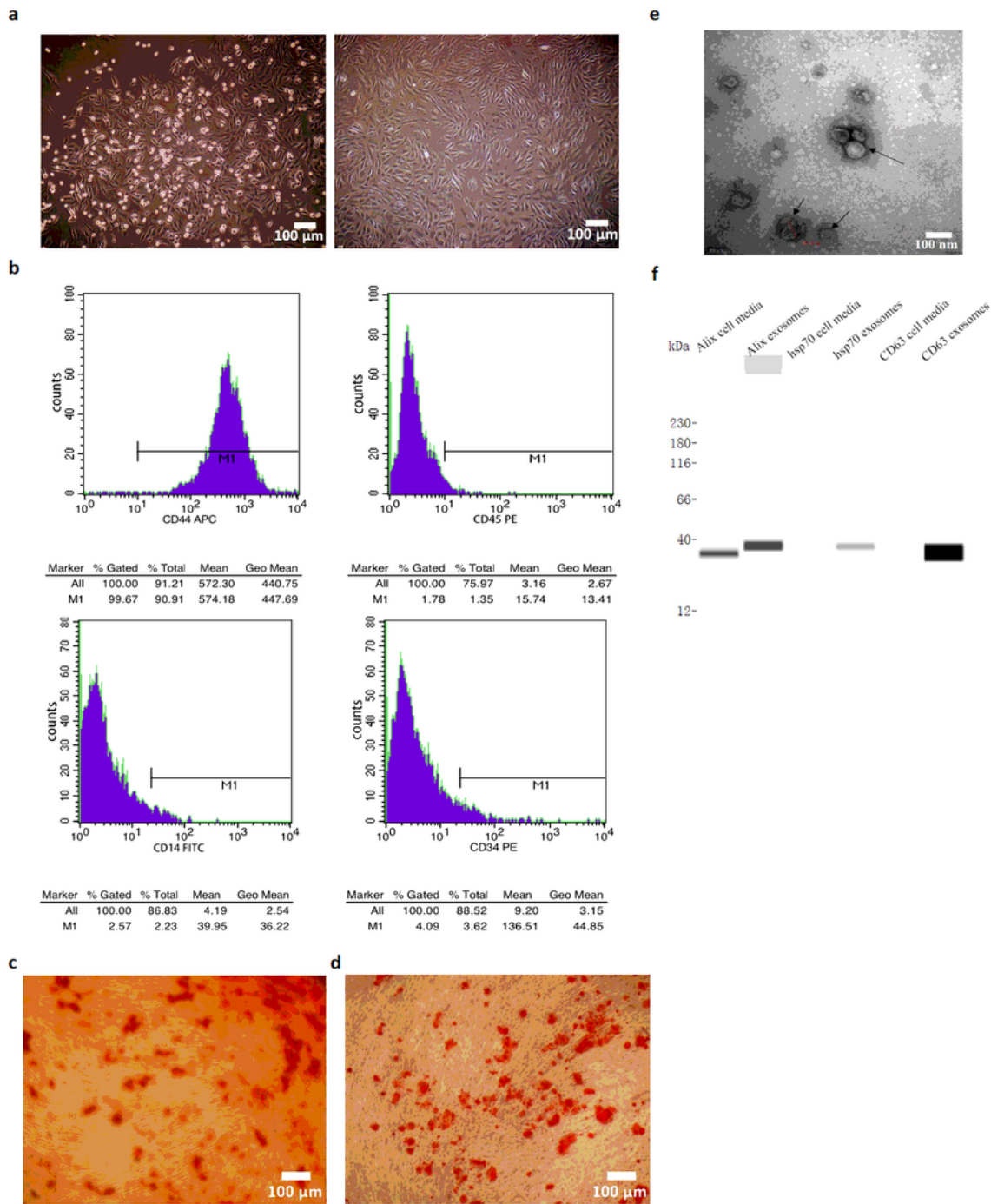


Figure 3

Effect of BMSCs-exos on the adherence, stretch and proliferation of BMSCs on the specimens. a Adhesion behavior of BMSCs on the titanium plates (bar = 100 μm). b Quantitative outcomes of BMSCs adhesion after incubation of 0.5, 1, and 4 h. c CCK-8 outcomes of BMSCs after incubation of 1, 2, and 3 days on the

titanium plates. d Representative staining images of F-actin (green) and nucleus (blue) after incubation of 1, 4, and 12 h (bar = 100 μm). * $p < 0.05$ compared to control group, ** $p < 0.01$ compared to control group, *** $p < 0.001$ compared to control group, **** $p < 0.0001$ compared to control group

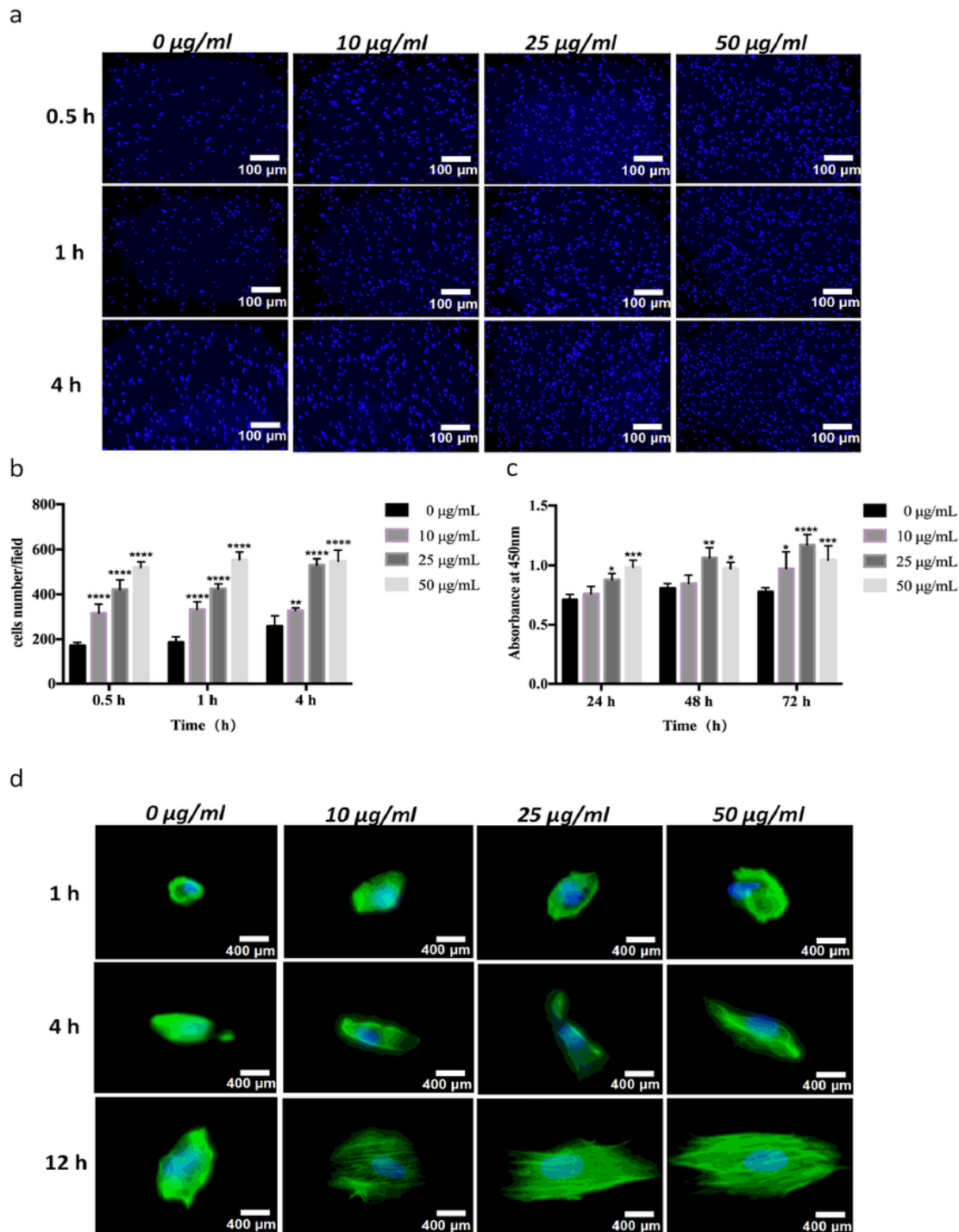


Figure 4

Detection of osteogenic correlation on titanium plates. a Representative images of ALP staining of BMSCs after osteogenic induction for 7 days and 14 days . b Quantitative outcomes of ALP staining area

after osteogenic induction for 7 days and 14 days. c Quantitative results of COL- α secretion by BMSCs after osteogenic induction for 7 and 14 days. d Representative images of Alizarin Red S staining of BMSCs after osteogenic induction for 21 days. *p < 0.05 compared to control group, **p < 0.01 compared to control group, ***p < 0.001 compared to control group, ****p < 0.0001 compared to control group

Supplementary Files

This is a list of supplementary files associated with this preprint. Click to download.

- [ARRIVEChecklist.pdf](#)
- [supplementaryinformation.pdf](#)